

## Copper(II) Ion-Doped Polyimide Composite for Nonenzymatic Electrochemical Hydrogen Peroxide Sensing

Lin Chen<sup>1,2</sup>, Yue Wang<sup>1,\*</sup>, Yasushi Hasebe<sup>3</sup>, Xi Yang<sup>1</sup>, Dandan Zhang<sup>1</sup>,  
Zhiqiang Zhang<sup>1</sup>, Zhizhi Hu<sup>1,\*</sup>

<sup>1</sup> School of Chemical Engineering, University of Science and Technology Liaoning, 185 Qianshan Middle Road, High-tech zone, Anshan, Liaoning, 114051, China.

<sup>2</sup> Department of Chemistry and Environmental Engineering, Yingkou Institute of Technology, Yingkou, Liaoning, 115014, China.

<sup>3</sup> Department of Life Science and Green Chemistry, Saitama Institute of Technology, 1690 Fusaiji, Fukaya, Saitama 369-0293, Japan.

\*E-mail: [wangyue@ustl.edu.cn](mailto:wangyue@ustl.edu.cn) (Yue Wang), [huzhizhi@163.com](mailto:huzhizhi@163.com) (Zhizhi Hu).

Received: 25 October 2018 / Accepted: 26 November 2018 / Published: 10 April 2018

---

A simple and facile nonenzymatic electrochemical sensor for the amperometric detection of H<sub>2</sub>O<sub>2</sub> was developed using a copper (II) ion-doped polyimide (PI)-modified glassy carbon electrode (GCE). The resulting Cu/PI-GCE exhibited sufficient electrocatalytic activity for both the reduction and oxidation of H<sub>2</sub>O<sub>2</sub> over a wide pH range. In the cathodic detection mode at -0.2 V vs. Ag/AgCl, the linear calibration range of H<sub>2</sub>O<sub>2</sub> was 0.01 mM to 20 mM, and the limit of detection was found to be 3.8 μM (S/N=3). In the anodic detection mode at +0.6 V vs. Ag/AgCl, the Cu/PI-GCE showed a wide linear range from 0.03 mM to 5 mM, and the limit of detection was determined to be 14.1 μM (S/N=3). In both detection modes, the response time was less than 4 s. The Cu/PI-GCE showed acceptable selectivity and was able to detect the presence of H<sub>2</sub>O<sub>2</sub> in tap water. Furthermore, the Cu/PI-GCE exhibited excellent reproducibility and long-term storage stability (under dry conditions).

---

**Keywords:** polyimide, copper ion, electrochemical sensor, nonenzymatic sensing, hydrogen peroxide

### 1. INTRODUCTION

The rapid and exact detection of hydrogen peroxide (H<sub>2</sub>O<sub>2</sub>) is necessary because it is not only an important byproduct of various oxidases but also an essential compound in food production and in clinical, pharmaceutical, sterilization and environmental analyses [1-5]. Among the various analytical methods for H<sub>2</sub>O<sub>2</sub> [6-10], electrochemical detection is popular owing to its low detection limit and low cost compared with those of other techniques and is widely applied for both enzymatic and nonenzymatic

sensors [11-14]. Because of the environmentally sensitive nature of enzymatic biosensors, nonenzymatic sensors have aroused great interest in recent years [15-17].

Transition metal materials are also promising for the development of nonenzymatic H<sub>2</sub>O<sub>2</sub> sensors because of their high electrochemical activity [18-22]. Various transition metal materials in different forms, such as TiO<sub>2</sub> [23], Cu<sub>2</sub>O [24], PdO [25], gold [26], and ZnO [27], have been applied in the electrochemical field. Among these transition metal materials, copper-based compounds, such as CuO nanorod bundles [28], Cu<sub>2</sub>O microcubes [29], Cu nanoparticles [30], and DNA-Cu complexes [31], have received much attention in recent years because of their excellent properties. However, relatively few reports have been found on the application of copper inorganic salt-based electrochemical sensors.

Polymer films have the characteristics of a light weight, a high specific strength, excellent physical and chemical stabilities, and a low cost [32-34] and have been applied in the electronics [35], energy [36], environmental [37], biological [38], and health care [39] fields. Among various polymer films, polyimide (PI) has a rigid-rod backbone and is frequently used as a coating layer and film adhered to a metal substrate.<sup>40</sup> In addition, the flexibility and stretchability of PI give it a wide range of applications for future electronics. In fact, PI films have been employed as flexible thermal microelectro mechanical system (MEMS) devices [41, 42] and humidity sensors [43, 44]. However, the intrinsic insulating property of PI restricts its application in the field of electrochemical sensors.

Recently, we used PI as a support matrix for electrochemical sensors to develop a carbon black and carbon nanotube hybrid composite-doped PI film-modified electrode for the simultaneous detection of ascorbic acid, dopamine and uric acid.<sup>45</sup> In this study, as another example of a PI-film-based electrochemical sensor, we report a copper (II) ion-doped PI (Cu/PI) film-modified glassy carbon electrode (GCE) for the nonenzymatic electrochemical detection of H<sub>2</sub>O<sub>2</sub>. Taking advantage of metal ions as catalysts and the physical and chemical stabilities of PI, the Cu/PI film-modified GCE (Cu/PI-GCE) exhibited highly sensitive, selective and stable electrocatalytic activity for the reduction and oxidation of H<sub>2</sub>O<sub>2</sub>. The combination of metal inorganic salts (CuSO<sub>4</sub>) and PI would enhance not only the conductivity of PI but also the reproducibility and long-term life of the sensor.

## 2. EXPERIMENTAL PROCEDURE

### 2.1. Materials and reagents

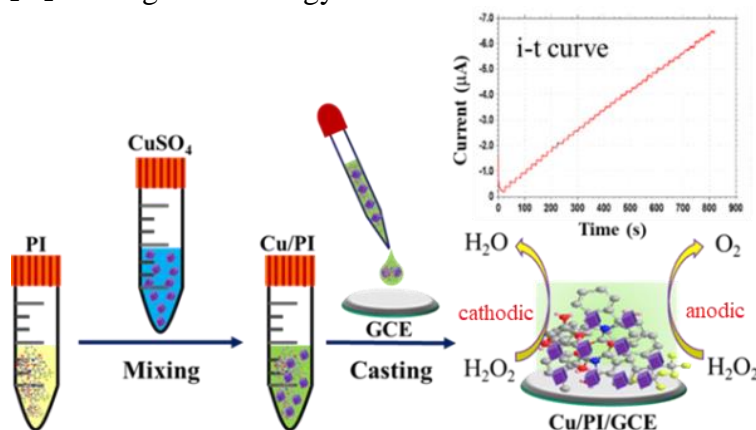
Copper sulfate (CuSO<sub>4</sub>), uric acid (UA), ascorbic acid (AA), glucose, fructose, sodium hydroxide (NaOH), N,N'-dimethylacetamide (DMAc), phosphoric acid, glacial acetic acid, boric acid and H<sub>2</sub>O<sub>2</sub> were obtained from Sinopharm Chemical Reagent Co., Ltd., China. DMAc was dried by anhydrous molecular sieves before use. A 0.1 M Britton-Robinson (BR) buffer (prepared by mixing 0.1 M NaOH and 0.1 M solutions of phosphoric acid, acetic acid, and boric acid) was used to prepare the electrolyte for the acidic, neutral and alkaline solutions. All other chemicals were of analytical grade and were used without further purification.

## 2.2. Apparatus

The morphologies of the surface of the PI-modified glassy carbon electrode (GCE, 3 mm diameter, Shanghai Chenhua, China) and Cu/PI-GCE were observed using field emission scanning electron microscopy (FE-SEM, SIGMA-HD, ZEISS, Germany) and atomic force microscopy (AFM, Being Nano-instruments CSPM-5500, BenYuan, China). Electrochemical measurements were performed with a CHI 750D workstation (Shanghai Chenhua, China). A conventional three-electrode system with the Cu/PI-GCE as the working electrode, a thin Pt wire as the counter electrode and Ag/AgCl (sat. KCl) as a reference electrode was employed in this study. All measurements were performed in air at room temperature, which was approximately 20°C.

## 2.3. Fabrication procedures of the Cu/PI-GCE

The preparation process of PI was previously reported [45]. The as-obtained PI (30 mg) was diluted in DMAc solvent (0.57 g) and sonicated for 30 min to make a homogeneous solution. The CuSO<sub>4</sub> solution was prepared by putting 15 mg of CuSO<sub>4</sub> into 0.5 mL of DMAc and sonicating the solution for 30 min. The PI solution was mixed with the CuSO<sub>4</sub> solution and sonicated for 30 min, which is referred to hereafter as the Cu/PI solution. The disk plane of the GCE was sequentially polished with 1.0, 0.3, and 0.05 μm α-alumina slurries to obtain a shiny surface. The cleaned electrode was rinsed and sonicated with distilled water and ethanol to remove any adhering alumina. Next, the GCE surface was coated by a casting Cu/PI solution (10 μL), and then the electrode was allowed to dry for 24 h at room temperature. The as-obtained sensor is referred to as the Cu/PI-GCE. The preparation procedure used to create the Cu/PI-GCE and the H<sub>2</sub>O<sub>2</sub> sensing methodology are shown in Scheme 1.



**Scheme 1.** Preparation procedure for the Cu/PI-GCE and H<sub>2</sub>O<sub>2</sub> sensing methodology.

## 3. RESULTS AND DISCUSSION

### 3.1. Surface morphology of the PI film-modified electrodes

The SEM and AFM images of the PI-modified GCE (PI-GCE) and the Cu-doped PI-modified GCE (Cu/PI-GCE) are shown in Fig. 1. The PI-GCE has a smooth surface (panels A and C). In contrast,

after doping with  $\text{CuSO}_4$ , a dispersed ball-shaped image was observed (panels B and D). These images indicate that the thickness and surface roughness are increased because of the inhomogeneity of the physical mixing of the Cu ions and PI. However, by successfully doping the PI-GCE with Cu ions, an improvement in the conductivity of the film can be expected.

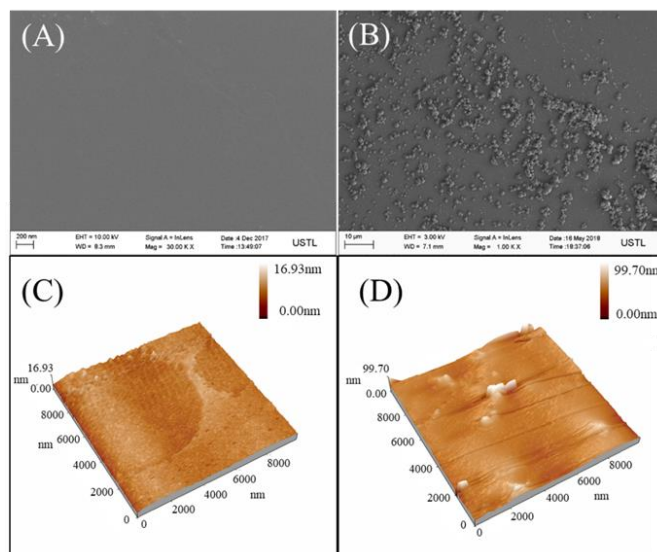
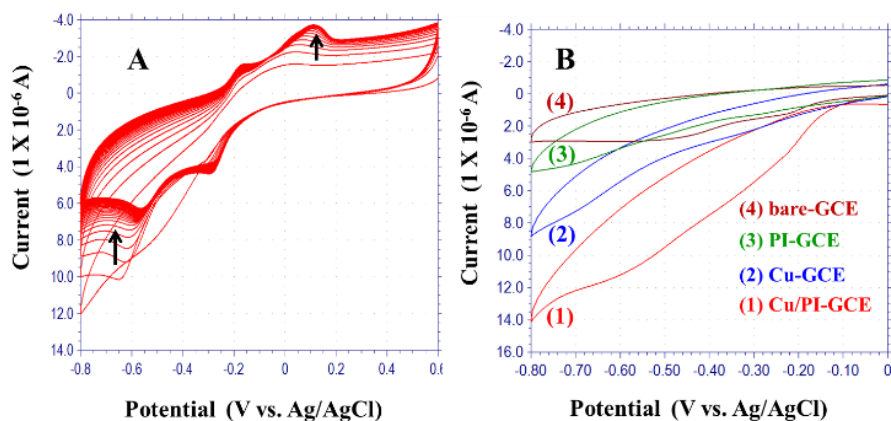


**Figure 1.** SEM and AFM images of the PI-GCE (A, C) and Cu/PI-GCE (B, D).

### 3.2. Electrochemical properties of the Cu/PI-GCE

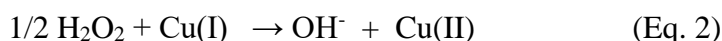
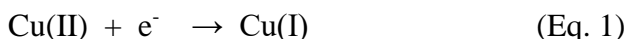
#### 3.2.1 Cathodic electrocatalytic activity of the Cu/PI-GCE toward $\text{H}_2\text{O}_2$

Fig. 2A shows the cyclic voltammetry response of the Cu/PI-GCE in a deoxygenated 0.1 M BR buffer (pH 9.0) during 100 repeated potential scans. Two separated oxidation peaks and reduction peaks were observed after several initial potential scans. Here, the two separated reduction peaks probably correspond to the stepwise one-electron reduction of  $\text{Cu(II)}$  to  $\text{Cu(I)}$  and  $\text{Cu(I)}$  to  $\text{Cu(0)}$ , whereas the two separated oxidation peaks likely correspond to the one-electron oxidation of  $\text{Cu(0)}$  to  $\text{Cu(I)}$  and of  $\text{Cu(I)}$  to  $\text{Cu(II)}$ . Another possibility is that different binding modes of Cu exist within the PI film, and two kinds of Cu ions with different environments lead to separated redox couples of  $\text{Cu(II)/Cu(I)}$ . The shape of the CVs was almost unchanged even after 100 additional repeated cyclic voltammetry scans (a total of 200 scans). Although the detailed electrochemical reaction mechanism is still unclear in this stage, at least it is safe to assume that the doped Cu ions maintain stable electrochemical properties even within the PI film.



**Figure 2.** (A) Cyclic voltammograms (CVs) of the Cu/PI-GCE in a deoxygenated 0.1 M BR buffer (pH 9.0). The potential scans were repeated 100 times. (The starting potential was +0.6 V). (B) CVs of the Cu/PI-GCE, Cu-GCE, PI-GCE, and bare-GCE in a deoxygenated 0.1 M BR buffer (pH 9.0) in the presence of a 5 mM  $\text{H}_2\text{O}_2$ .

To confirm the electrocatalytic activity of the Cu/PI-GCE toward  $\text{H}_2\text{O}_2$ , we next measured the CVs in the presence of  $\text{H}_2\text{O}_2$  by using 4 electrodes: (1) the Cu/PI-GCE, (2) the Cu-GCE, (3) the PI-GCE, and (4) the bare-GCE. In the case of the Cu/PI-GCE, a large cathodic current appeared from -0.15 V to -0.7 V. This potential range almost corresponds to the reduction potential range of the Cu/PI-GCE shown in Fig. 2A, which suggests that the Cu ions act as electrocatalysts for  $\text{H}_2\text{O}_2$  reduction according to the following schemes.



However, for the Cu-GCE, although a small cathodic current can be observed in the same potential region, the magnitude of the current is much smaller than that of the Cu/PI-GCE. These results clearly indicate that Cu ions doped in PI can act as an efficient electrocatalyst for  $\text{H}_2\text{O}_2$  reduction.

### 3.2.2 Anodic electrocatalytic activity of the Cu/PI-GCE toward $\text{H}_2\text{O}_2$

To confirm the electrocatalytic activity of the Cu/PI-GCE toward  $\text{H}_2\text{O}_2$ , cyclic voltammetry measurements of the Cu/PI-GCE with different concentrations of  $\text{H}_2\text{O}_2$  were performed in a 0.1 M deoxygenated BR buffer solution (pH 9.0) (Fig. 3). Both the cathodic and anodic currents increased clearly with increasing concentrations of  $\text{H}_2\text{O}_2$ , which suggests the possibility of both anodic and cathodic determination of  $\text{H}_2\text{O}_2$  by a single electrode. In the case of anodic detection by the Cu/PI-GCE, we speculate the following mechanism.



$\text{H}_2\text{O}_2$  reduces  $\text{Cu}^{2+}$  to  $\text{Cu}^+$ , and the oxidation current due to Eq. 4 can be monitored by the catalytic current. These results clearly support our speculation that Cu ions doped within a PI film play a crucially important role in the generation of this electrocatalytic activity of the Cu/PI-GCE.

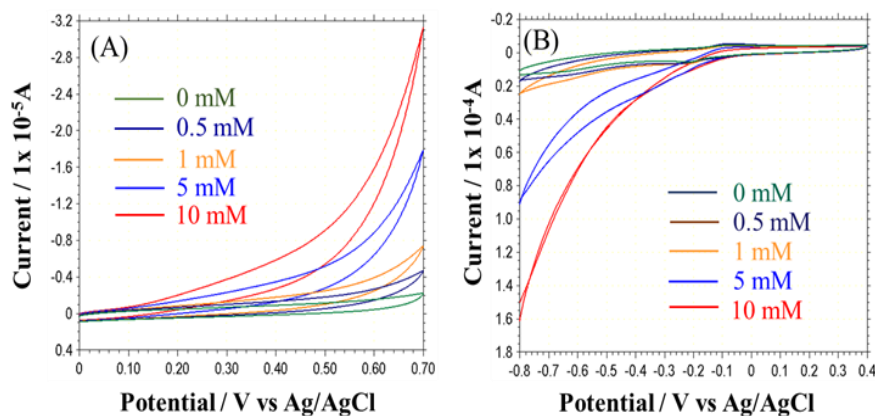


**Figure 3.** (A) Cyclic voltammograms (CVs) of the Cu/PI-GCE in different concentrations of  $\text{H}_2\text{O}_2$  (0–10 mM) in the positive potential range; the starting potential was 0 V. (B) CVs of the Cu/PI-GCE in different concentrations of  $\text{H}_2\text{O}_2$  (0–10 mM) in the negative potential range; the starting potential was +0.4 V.  $[\text{CuSO}_4] = 30 \text{ mg mL}^{-1}$ . A deoxygenated 0.1 M BR buffer (pH 9.0) was used as the electrolyte.

### 3.3 Optimization of the measurement and preparation conditions

Next, we optimized various operational conditions and preparation conditions of the Cu/PI-GCE-based nonenzymatic  $\text{H}_2\text{O}_2$  sensor. Fig. 4A illustrates the effect of the applied potential upon the steady-state cathodic current responses to a 1 mM  $\text{H}_2\text{O}_2$  solution (red) and background current (blue). Although the  $\text{H}_2\text{O}_2$  response itself increased with decreasing potential, the background current from the electrochemical reduction of the dissolved oxygen in the electrolyte substantially increased, and the baseline drift was also extensive when the negative potential was greater than -0.3 V. Thus, an applied potential of -0.2 V was selected for the following cathodic  $\text{H}_2\text{O}_2$  sensing experiments.

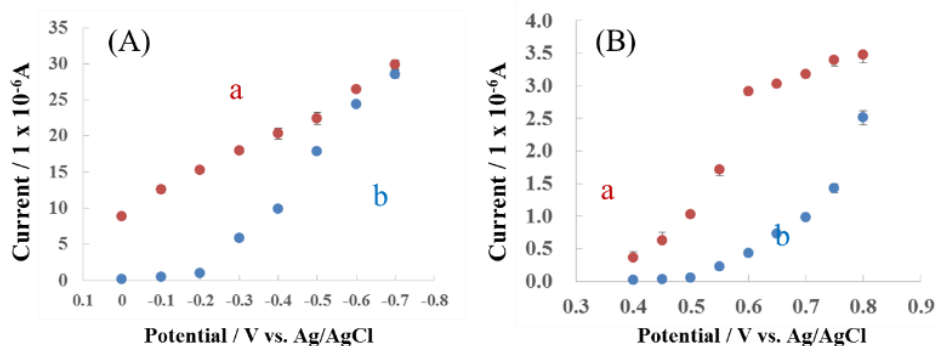


**Figure 4.** (A) Effect of the applied potential on the steady-state cathodic current response to a 1 mM  $\text{H}_2\text{O}_2$  solution (a) and background current (b). (B) Effect of the applied potential on the anodic current response to a 1 mM  $\text{H}_2\text{O}_2$  solution (a) and background current (b). The electrolyte is air-saturated 0.1 M BR buffer pH 9.0.  $[\text{CuSO}_4] = 15 \text{ mg/mL}$ .

A similar experiment was performed for the anodic response in the potential range from +0.4 V to +0.8 V (Fig. 4B). Although the anodic catalytic current increased with potential, the noise level also

increased, and the drift of the baseline was large in the high-potential region. Therefore, we selected +0.6 V for the following anodic H<sub>2</sub>O<sub>2</sub> sensing experiments.

In some nonenzymatic H<sub>2</sub>O<sub>2</sub> sensors [21, 46], alkaline conditions are essential to obtain sufficient responses. However, for common and universal applications, such restricted conditions are not preferable, and detection in a wide pH range is ideal. Therefore, the effect of the pH of the electrolyte on the H<sub>2</sub>O<sub>2</sub> response was evaluated (Fig. 5A). The applied potential was fixed at +0.6 V for anodic detection and -0.2 V for cathodic detection, respectively. In both cases, a relatively high pH (8 to 12) seemed to be suitable, and the Cu/PI-GCE sensor could be used in both neutral and acidic solutions. This feature is one of the advantages over other nonenzymatic electrochemical H<sub>2</sub>O<sub>2</sub> sensors [21, 46], and the sensor can be expected to have future applications in environmental and biological samples. As described above, the Cu ions are the key catalysts of this system. As such, the effect of the concentration of CuSO<sub>4</sub> during the preparation of the H<sub>2</sub>O<sub>2</sub> response was studied next (Fig. 5B). The concentrations of 20 mg/mL and 15 mg/mL CuSO<sub>4</sub> gave the best results for the anodic and cathodic determination of H<sub>2</sub>O<sub>2</sub>, respectively. The large capacity of PI gives a free volume combination for the CuSO<sub>4</sub>.

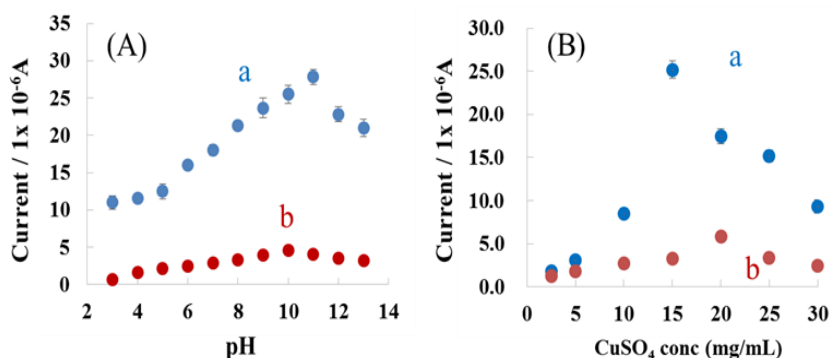


**Figure 5.** (A) Effect of the pH on the cathodic current (a, applied potential -0.2 V) and anodic current (b, applied potential +0.6 V) responses to a 1 mM H<sub>2</sub>O<sub>2</sub> solution. [CuSO<sub>4</sub>] = 15 mg/mL. (B) Effect of the CuSO<sub>4</sub> concentration used for the preparation of the Cu/PI-GCE on the responses of the cathodic current (a) and anodic current (b) to a 1 mM H<sub>2</sub>O<sub>2</sub> solution.

### 3.4 Amperometric response characteristics of the Cu/PI-GCE to H<sub>2</sub>O<sub>2</sub>

The amperometric oxidation and reduction current curves obtained under the optimized conditions for a series of H<sub>2</sub>O<sub>2</sub> solutions with different concentrations are shown in Figs. 6A and 7A, respectively. Figs. 6B and 7B show the plots of the oxidation and reduction currents toward the concentration of H<sub>2</sub>O<sub>2</sub>. The calibration curve for the reduction of H<sub>2</sub>O<sub>2</sub> in the range of 1.0 × 10<sup>-5</sup> mol L<sup>-1</sup> to 2.0 × 10<sup>-2</sup> mol L<sup>-1</sup> is  $I (\mu\text{A}) = 0.1584 + 13.2798 C (\mu\text{mol L}^{-1})$  with a correlation coefficient of 0.9956, and the detection limit was found to be 3.8 μmol L<sup>-1</sup> (S/N=3). The calibration curve for the oxidation of H<sub>2</sub>O<sub>2</sub> in the range of 3.0 × 10<sup>-5</sup> mol L<sup>-1</sup> to 5.0 × 10<sup>-3</sup> mol L<sup>-1</sup> is  $I (\mu\text{A}) = 0.0764 + 3.782 C (\mu\text{mol L}^{-1})$  with a correlation coefficient of 0.9997, and the detection limit was found to be 14.1 μmol L<sup>-1</sup> (S/N=3). The performances were very comparable to those for the amperometric sensors for H<sub>2</sub>O<sub>2</sub> that have been recently reported (Table 1) [18, 21, 24, 46, 48-49].

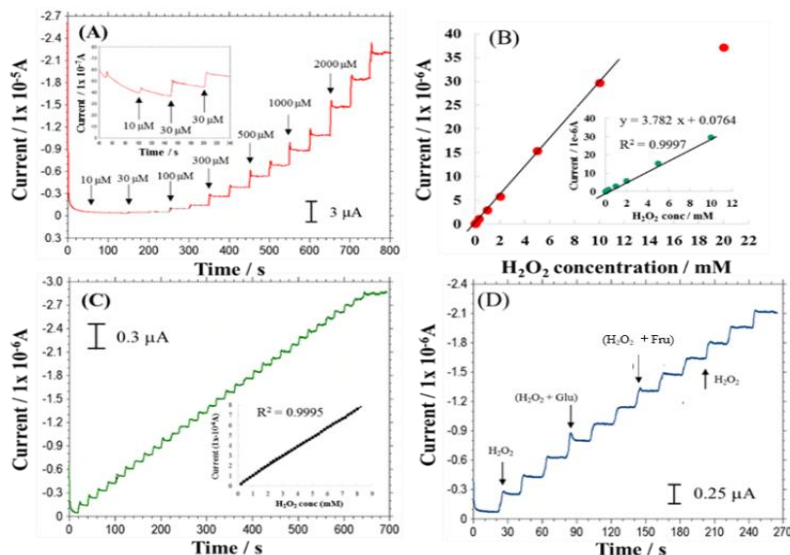


**Figure 6.** (A) Steady-state anodic current responses of the Cu/PI-GCE sensor for successive additions of different concentrations of H<sub>2</sub>O<sub>2</sub>. (Inset is the enlargement of the lower concentration region). (B) Calibration curves of the H<sub>2</sub>O<sub>2</sub> obtained with the anodic mode. The inset is an enlargement of the linear part of the calibration curve. (C) The amperometric response of the Cu/PI-GCE for successive additions of 0.2 mM H<sub>2</sub>O<sub>2</sub>. The inset is the linear relationship between the H<sub>2</sub>O<sub>2</sub> concentration and the current response. (D) The amperometric responses of the Cu/PI-GCE for successive additions of 0.2 mM H<sub>2</sub>O<sub>2</sub> and the mixture of 0.2 mM H<sub>2</sub>O<sub>2</sub> and 0.2 mM possible interferences (i.e., glucose, fructose). All measurements were carried out at an applied potential of +0.6 V in an air-saturated 0.1 M BR buffer (pH 11). [CuSO<sub>4</sub>] = 20 mg mL<sup>-1</sup>.

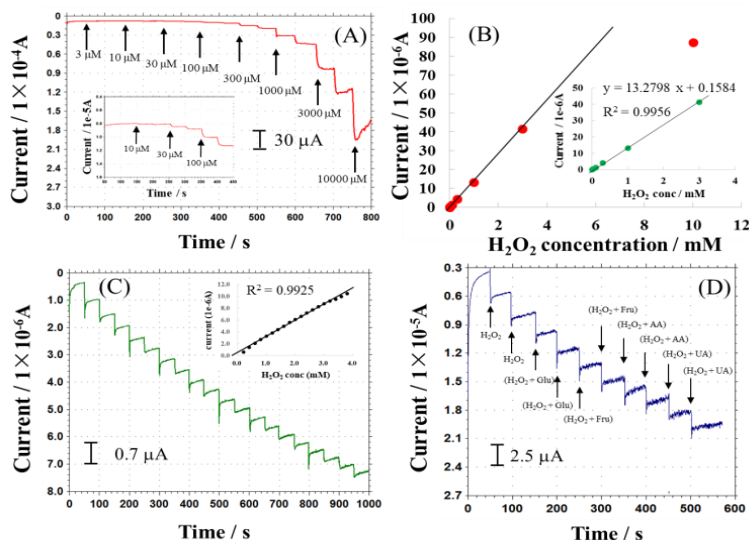


**Figure 7.** (A) Steady-state cathodic current response of the Cu/PI-GCE sensor for successive additions of different concentrations of H<sub>2</sub>O<sub>2</sub>. (Inset is the enlargement of the lower concentration region). (B) Calibration curves of the H<sub>2</sub>O<sub>2</sub> obtained with the cathodic mode. The inset is an enlargement of the linear part of the calibration curve. (C) The amperometric response of the Cu/PI-GCE to a 0.2 mM H<sub>2</sub>O<sub>2</sub> solution. The inset shows the linear relationship of the H<sub>2</sub>O<sub>2</sub> concentration and the current response. (D) The amperometric responses of the Cu/PI-GCE for the successive additions of 0.2 mM H<sub>2</sub>O<sub>2</sub> and the mixture of 0.2 mM H<sub>2</sub>O<sub>2</sub> and 0.2 mM possible interferences (i.e., glucose, fructose, UA, and AA). All measurements were carried out at -0.2 V vs. Ag/AgCl in an air-saturated 0.1 M BR buffer (pH 10). [CuSO<sub>4</sub>] = 15 mg mL<sup>-1</sup>.

Figs. 6C and 7C show the oxidation and reduction current responses to successive additions of  $\text{H}_2\text{O}_2$  under the optimized conditions. Both the oxidative and the reductive current increase to reach a stable plateau within 4 s after adding the  $\text{H}_2\text{O}_2$  into the electrolyte; this result indicates that the permeation and diffusion of the  $\text{H}_2\text{O}_2$  within the Cu/PI layer is sufficiently fast, which leads to a rapid response. The Cu/PI-GCE exhibited good repeatability with a relative standard deviation (RSD) of 5.25% and 6.36% for the anodic and cathodic detection, respectively, after 15 successive measurements.

### 3.5 Selectivity and stability of the Cu/PI-GCE

Selectivity is an important parameter for nonenzymatic  $\text{H}_2\text{O}_2$  sensors. The effect of the various potentially interfering substances was tested to determine the selectivity of the present sensor. As shown in Figs. 6D and 7D, even at an applied potential of +0.6 V and -0.2 V, the current responses from the interferents are below 95.8% and 90.2%, respectively. These results indicate that the Cu/PI-GCE sensor gives a rather favorable selectivity to  $\text{H}_2\text{O}_2$ .

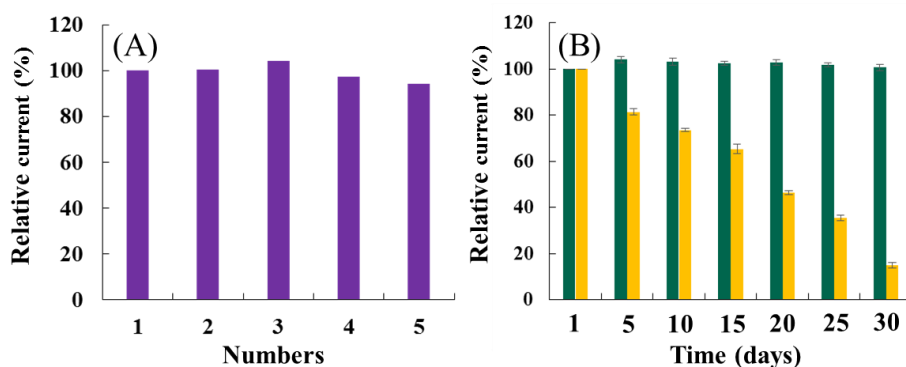


**Figure 8.** (A) The reproducibility of five independent Cu/PI-GCE sensors to 0.2 mM  $\text{H}_2\text{O}_2$ . (B) Long-term stability of the Cu/PI-GCE to a 0.2 mM  $\text{H}_2\text{O}_2$  solution. The applied potential is + 0.6 V vs. Ag/AgCl, 0.1 M BR buffer solution (pH 9),  $n=3$ .

To study the reproducibility of the electrode preparation, 5 electrodes were prepared under the same conditions; the reproducibility was determined to be 1.9% for these electrodes. In addition, stability is another essential parameter for the practical usage of nonenzymatic sensors. The long-term stability of the Cu/PI-GCE was examined by detecting a 0.2 mM  $\text{H}_2\text{O}_2$  solution at + 0.6 V 10 times with an interval of 5 days. When not in use, the sensor was placed in the lab in room temperature air. In the case of the Cu/GCE (without PI), the response was decreased less than 15% after 1 month of storage (drift rate: 2.9%/day). Compared with the stability characteristics of the Cu/GCE, the recorded amperometric response of the Cu/PI-GCE exhibited almost no decline, and, even after 1 month of storage, 100.6% of the initial current was maintained (Fig. 8B). Therefore, this satisfactory stability performance is related to the stable characteristics of PI. Thus, it could be concluded that the Cu/PI-GCE sensor is highly stable and would function reasonably well for approximately 1 month. These results are better than other copper-based nonenzymatic  $\text{H}_2\text{O}_2$  sensors that are prepared by complicated fabrication procedures [4, 21].

**Table 1.** Comparison between the sensors investigated in this study and other H<sub>2</sub>O<sub>2</sub> sensors

Electrode material	Linear range (mM)	LOD (mM)	Sensitivity ( $\mu\text{A mM}^{-1} \text{cm}^{-2}$ )	Ref
FeS (F4)	0.5-20.5	0.15	36.4	15
Cu <sub>2</sub> OMS-rGO	0.005-2.775	10.8	Not given	18
Cu@CuO/GCE	0.003-8	0.21	Not given	21
Cu <sub>2</sub> O/GNs/GCE	0.3-7.8	20.8	Not given	24
Nafion/NPC-CB/GCE	0.003-2.338	1.2	3.91	46
CuO/rGO/Cu <sub>2</sub> O/Cu	0.5-9.7	0.05	366.2	47
GO-Ag nanocomposite	0.1-11	0.028	0.1218	48
Co@Pt NPs	1.0-300	0.3	2.26	49
Cu/PI-GCE (anodic)	0.01-20	0.0038	188.0	This
Cu/PI-GCE (cathodic)	0.03-5	0.014	35.5	work

Cu<sub>2</sub>OMS = cuprous oxide microspheres; rGO = reduced graphene oxide; Cu<sub>2</sub>O = cuprous oxide nanocubes; GNs = graphene nanosheets; GCE = glassy carbon electrode; NPC = nanoporous copper; CB = carbon black; and FeS (F<sub>4</sub>) = ferrous sulfide nanosheets.

### 3.6 Real sample analysis

The practical application is an important characteristic with which to judge the performance of a sensor. H<sub>2</sub>O<sub>2</sub> is frequently used for sterilization of bottles of drinking water. Thus, the determination of residual H<sub>2</sub>O<sub>2</sub> in drinking water is important in the food industry. To demonstrate the feasibility of the Cu/PI-GCE sensor for routine analysis, it was used to determine H<sub>2</sub>O<sub>2</sub> in real drinking water. The amperometric detection of H<sub>2</sub>O<sub>2</sub> in drinking water samples was carried out by the standard addition method, and the results are shown in Table 2. The results obtained by the Cu/PI-GCE were in satisfactory agreement with those obtained by the standard titration method.

**Table 2.** Analytical results for H<sub>2</sub>O<sub>2</sub> in drinking water

Number	Measured by the proposed H <sub>2</sub> O <sub>2</sub> biosensor				
	Detected (mM)	Added (mM)	Found (mM)	RSD <sup>a</sup> (%)	Recovery (%)
1	Not found	50	51.5	4.8	103.0
2	Not found	100	105.0	3.9	105.0
3	Not found	200	213.0	3.5	106.5

<sup>a</sup> RSD (%) calculated from three separate experiments

## 4. CONCLUSIONS

A new copper ion-doped polyimide-modified electrochemical sensor was demonstrated through the simple physical one-step adsorption method. In the electrochemical measurements, the as-obtained Cu/PI-GCE exhibited good electrocatalytic activity toward both the oxidation and reduction of hydrogen

peroxide. The Cu/PI-GCE showed good linear response, a rapid response time, a low detection limit, high selectivity, good operational stability and excellent long-term storage stability. The novel Cu/PI composite will offer many potential applications in various electronics, including biosensors, bioelectronics devices and biocatalysts.

#### ACKNOWLEDGEMENTS

The authors gratefully acknowledge the financial support provided by the Natural Science Foundation of Liaoning Province (No. 20170540464), the Department of Education of Liaoning (No. 2017LNQN05) and the Foundation of University of Science and Technology, Liaoning (No. 2016RC12).

#### References

1. T. Ruzgas, E. Csöregi, J. Emneus, L. Gorton and G. Marko-Varga, *Anal. Chim. Acta*, 330 (1996) 123.
2. N. V. Klassen, D. Marchington and H. C. E. McGowan, *Anal. Chem.*, 66 (1994) 2921.
3. G. S. Cao, P. L. Wang, X. Li, Y. Wang, G. L. Wang and J. P. Li, *B. Mater. Sci.*, 38 [2015] 163.
4. Z. K. Yan, J. W. Zhao, L. R. Qin, F. Mu, P. Wang and X. N. Feng, *Microchim. Acta*, 180 (2013) 145.
5. M. Schaferling, D. B. M. Grogel and S. Schreml, *Microchim. Acta*, 174 (2011) 1.
6. U. Pinkernell, S. Effkemann and U. Karst, *Anal. Chem.*, 69 (1997) 3623.
7. D. E. Achatz, R. J. Meier, L. H. Fishcher and O. S. Wolfbeis, *Angew. Chem. Int. Ed.*, 50 (2011) 260.
8. A. E. Albers, V. S. Okreglak and C. J. Chang, *J. Am. Chem. Soc.*, 128 (2006) 9640.
9. M. Giorgetti, D. Tonelli, M. Berrettoni, G. Aquilanti and M. Minicucci, *J. Solid State Electrochem.*, 18 (2014) 965.
10. T. R. Holm, G. K. George and M. J. Barcelona, *Anal. Chem.*, 59 (1987) 582.
11. Y. Wang, K. J. Zhao, D. P. Tao, F. G. Zhai, H. B. Yang and Z. Q. Zhang, *RSC Adv.*, 8 (2018) 5013.
12. X. M. Chen, G. H. Wu, Z. X. Cai, M. Oyama and X. Chen, *Microchim. Acta*, 181 (2014) 689.
13. C. S. Pundir, R. Deswal and V. Narwal, *Bioproce. Biosyst. Eng.*, 41 (2018) 313.
14. Y. Wang and Y. Hasebe, *Anal. Sci.*, 27 (2011) 401.
15. J. Y. Jin, W. Q. Wu, H. Min, H. M. Wu, S. F. Wang, Y. Ding and S. J. Yang, *Microchim. Acta*, 184 (2017) 1389.
16. B. Zhao, Z. Liu, W. Fu and H. Yang, *Electrochem. Commun.*, 27 (2013) 1.
17. G. George and S. Anandhan, *Thin. Solid. Films*, 610 (2016) 48.
18. J. W. Ding, W. Sun, G. Wei and Z. Q. Su, *RSC. Adv.*, 5 (2015) 35338.
19. X. D. Sui, J. Y. Liu, S. T. Zhang, J. Yang and J. Y. Hao, *Appl. Surf. Sci.*, 439 (2018) 24.
20. F. Y. Xie, X. Q. Cao, F. L. Qu, A. M. Asiri and X. P. Sun, *Sensor. Actuat. B-Chem.*, 255 (2018) 1254.
21. H. Y. Song, C. H. Ma, L. H. You, Z. Y. Cheng, X. H. Zhang, B. S. Yin, Y. N. Ni and K. Q. Zhang, *Microchim. Acta*, 182 (2015) 1543.
22. Y. B. Zhou, G. Yu, F. F. Chang, B. N. Hu and C. J. Zhong, *Anal. Chim. Acta*, 757 (2012) 56.
23. P. Si, S. J. Ding, J. Yuan, X. W. Lou and D. H. Kim, *ACS. Nano*, 5 (2011) 7617.
24. M. M. Liu, R. Liu and W. Chen, *Biosens. Bioelectron.*, 45 (2013) 206.
25. Y. Q. Zhang, W. X. Yang, Y. Z. Wang, J. B. Jia and J. G. Wang, *Microchim. Acta*, 180 (2013) 1085.
26. R. Ning, W. B. Lu, Y. W. Zhang, X. Y. Qin, Y. L. Lou, J. M. Hu, A. M. Asiri, A. O. Al-Youbi and X. Sun, *Electrochim. Acta*, 60 (2012) 13.
27. Q. Wang and J. B. Zheng, *Microchim. Acta*, 169 (2010) 361.

28. C. Batchelor-McAuley, Y. Du, G. G. Wildgoose and R. G. Compton, *Sensor. Actuat. B-Chem.*, 135 (2008) 230.
29. L. Zhang, H. Li, Y. H. Ni, J. Li, K. M. Liao and G. C. Zhao, *Electrochem. Commun.*, 11 (2009) 812.
30. T. Wang, J. S. Hu, W. Yang and H. M. Zhang, *Electrochem. Commun.*, 10 (2008) 814.
31. Y. Wang, W. Z. Wei, J. X. Zeng, X. Y. Liu and X. D. Zeng, *Microchimica. Acta*, 160 (2008) 253.
32. H. Deng, L. Lin, M. Z. Ji, S. M. Zhang, M. B. Yang and Q. Fu, *Prog. Polym. Sci.* 39 (2014) 627.
33. X. H. Li, L. B. Shao, N. Song and P. Ding, *Compos. Part. A-Appl. S.*, 88 (2016) 305.
34. G. L. Song, Y. Zhang, D. M. Wang, C. H. Chen, H. W. Zhou, X. G. Zhao and G. D. Dang, *Polymer* 54 (2013) 2335.
35. S. Joo, B. Kim, J. An, M. Park, S. Seo, J. Y. Park and J. Bae, *J. Mater. Sci.*, 53 (2018) 9316.
36. L. Ding, G. Xu, Q. Ge, T. Wu, F. Yang and M. Xiang, *Chinese. J. Polym. Sci.*, 36 (2018) 536.
37. C. M. Zhang, W. Song, X. C. Zhang, R. Li, S. J. Zhao and C. M. Fan, *J. Mater. Sci.*, 53 (2018) 9429.
38. Z. Q. Wang, J. Ni and D. R. Gao, *Friction*, 6 (2018) 183.
39. H. Lee, M. J. Glasper, X. D. Li, J. A. Nychka, J. Batcheller, H. J. Chung and Y. Chen, *J. Mater. Sci.*, 53 (2018) 9026.
40. T. Matsuura, Y. Hasuda, S. Nishi and N. Yamada, *Macromolecules*, 24 (1991) 5001.
41. M. Shikida, Y. Niimi and S. Shibata, *Microsyst. Technol.*, 23 (2017) 677.
42. W. Hasenkamp, D. Forchelet, K. Pataky, J. Villard, H. V. Lintel, A. Bertsch, Q. Wang and P. Renaud, *Biomed. Microdevices*, 14 (2012) 819.
43. Y. Lin, Y. Gong, Y. Wu and H. J. Wu, *Photonic. Sensors* 5 (2015) 60.
44. D. Z. Zhang, H. Y. Chang and R. H. Liu, *J. Electron. Mater.*, 45 (2016) 4275.
45. P.H. Li, C.Y. Wang, G. Li and J.M. Jiang, *Polym. Bull.*, 64 (2010) 127.
46. L. Mei, P. C. Zhang, J. Y. Chen, D. D. Chen, Y. Quan, N. Gu, G. H. Zhang and R. J. Cui, *Microchim. Acta*, 183 (2016) 1359.
47. C. J. Zhao, X. Wu, P. W. Li, C. H. Zhao and X. Z. Qian, *Microchim. Acta*, 184 (2017) 2341.
48. M. M. Shahid, P. Rameshkumar and N. M. Huang, *Microchim. Acta*, 183 (2016) 911.
49. H. Mei, W. Wu, B. Yu, Y. Li, H. Wu, S. Wang and Q. Xia, *Microchim. Acta*, 182 (2015) 1869.